

## Mechanism and numerical simulation of a rapid deep-seated landslide in Van Hoi reservoir, Vietnam

Pham Van Tien<sup>1,2</sup>, Le Hong Luong<sup>3</sup>, Tran Thanh Nhan<sup>4</sup>, Nguyen Quoc Phi<sup>5,\*</sup>, Trong Trinh Phan<sup>2,6</sup>, Dinh Thi Quynh<sup>1</sup>, Dao Minh Duc<sup>2</sup>, Nguyen Chau Lan<sup>7</sup>, Nguyen Hai Cuong<sup>4</sup>

<sup>1</sup>*Institute of Geotechnology and Environment, Hanoi, Vietnam*

<sup>2</sup>*Institute of Geological Sciences, Vietnam Academy of Science and Technology, Hanoi, Vietnam*

<sup>3</sup>*Institute of Transport Science and Technology, Hanoi, Vietnam*

<sup>4</sup>*University of Sciences, Hue University, Hue City, Vietnam*

<sup>5</sup>*University of Mining and Geology, Hanoi, Vietnam*

<sup>6</sup>*Royal Academy for Overseas Sciences, Brussels, Belgium*

<sup>7</sup>*University of Transport and Communications, Hanoi, Vietnam*

Received 30 March 2023; Received in revised form 26 June 2023; Accepted 10 July 2023

### ABSTRACT

At approximately 5:00 AM on December 16, 2016, a rapid and deep-seated landslide was triggered by intense rainfall in the Van Hoi irrigation reservoir in Binh Dinh province, Vietnam. The landslide generated an impulsive wave with a height of approximately 20 m, resulting in severe damage to the reservoir operation station. This study investigated the mechanisms behind the landslide's initiation and simulated its initiation and motion processes through site surveys, ring shear tests, and the LS-RAPID simulation model. The physical tests were conducted on two soil samples from the sliding zone to examine the landslide mechanism. The results indicated that only sample 2 (a sand sample of completely weathered gneiss rock) showed a high level of landslide mobility due to its liquefaction phenomena resulting in a rapid pore water pressure development and a significant strength loss.

In contrast, sample 1 (a silty sand sample of residual soils) did not exhibit this behavior due to its high shear resistance value at a steady state. The findings suggest that the sliding plane of the Van Hoi landslide formed in the completely weathered gneiss layer, and the high mobility level of sample 2 is primarily responsible for its rapid movement. Notably, the LS-RAPID model successfully reproduced the landslide process using the geotechnical properties obtained in the ring shear experiments. The simulation showed that the Van Hoi deep-seated landslide was initiated from the lower middle slope at a critical value of 0.55 for the pore water pressure ratio and traveled at a high velocity of approximately 37.0 m/s. The consistency between the computer simulation results and the on-site evidence and recorded data highlights the reliability of the LS-RAPID model as a tool for assessing landslide hazards.

*Keywords:* Deep-seated landslide, rainfall, pore water pressure, mobility, numerical simulation, Van Hoi reservoir, Vietnam.

### 1. Introduction

Vietnam has one of the world's largest dam and reservoir systems, with about 750

classified as medium or large dam reservoirs among over 7,000 dams (W.B., 2022). One notable reservoir in this system is the Van Hoi dam reservoir in An Tin commune, Hoai An district, Binh Dinh province. Since its establishment in 2003, the Van Hoi Reservoir

\*Corresponding author, Email: [nguyenquocphi@humg.edu.vn](mailto:nguyenquocphi@humg.edu.vn)

has played a vital role in irrigating an expansive area of 2.106 hectares. As a substantial irrigation dam, it features a 562 m long river-blocking dam and reaches a maximum height of 25 m, offering a storage volume capacity of 14.5 million cubic meters. With the dam crest and crown wall measuring 47.0 m and 47.8 m, respectively, the reservoir ensures a normal water surface of 44.0 m and a maximum water surface of 45.15 m (MARD, 2005). Unfortunately, the Van Hoi

reservoir's long-term sustainable operation and storage capacity was severely affected by sedimentation resulting from numerous landslides following the 2016 rainy season. The reservoir sedimentation has also affected the agricultural livelihoods of hundreds of downstream households. The geological map indicating the location of the study site and an unmanned aerial vehicle's photo showing the Van Hoi reservoir sedimentation due to landslides are shown in Fig. 1.

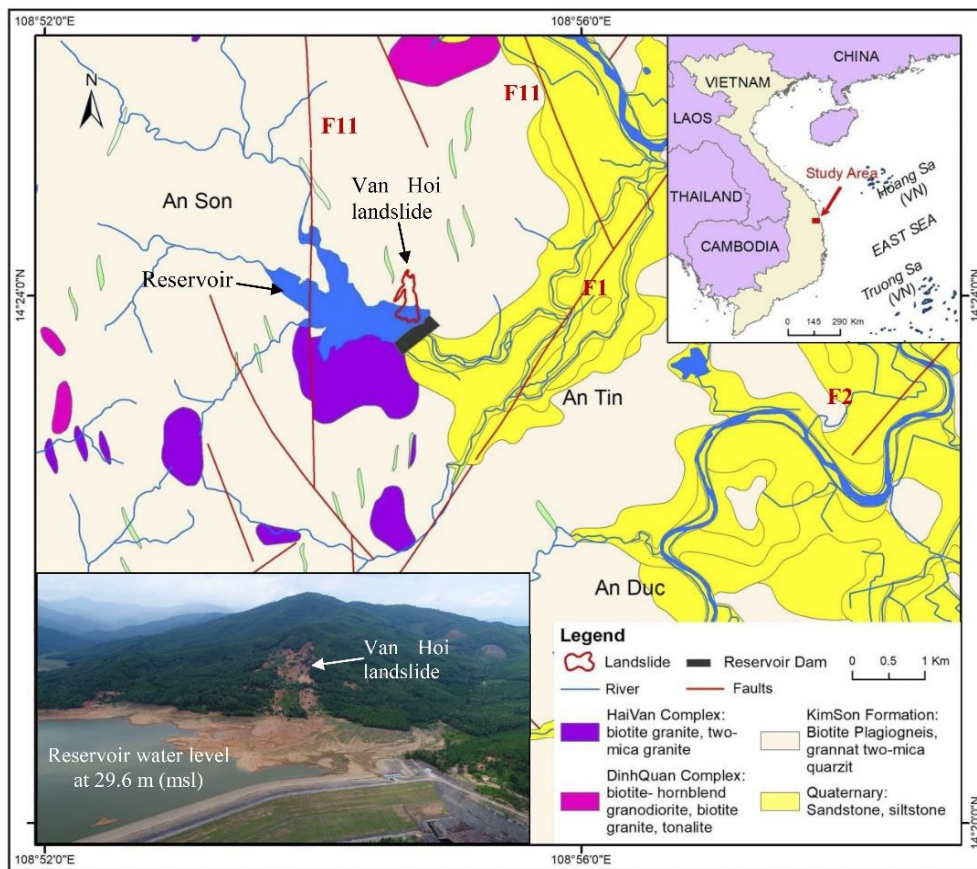


Figure 1. Geological map (scale 1:50.000) of the Van Hoi reservoir

The deep-seated landslide-induced tsunami wave was the most significant event among the numerous mass movements triggered by intense precipitation on December 16, 2016, in the Van Hoi reservoir (Fig. 2a). It caused significant damage to the dam reservoir and its mechanical components (Figs. 2b).

The rain-induced landslide initiated on the slope opposite the left abutment of the dam and traveled a distance of 300 m from the slope toe to the spillway gate. According to an interview with the on-duty staff at the operation house, the downslope movement took place on the site, followed by a loud

sound. Surprisingly, the landslide generated a highly impulsive water wave, resembling a tsunami, with a height of approximately 20 m. The high-pressure water blast, lasting for tens of seconds, struck the operation house and the abutment, causing extensive damage, but also broke two electricity poles and partly destroyed five others located along the dam crest. The water mass from the landslide-

induced tsunami led to water inundation in the operation house and scattered erosion along the stone embankment within the lake and in the lower part of the dam (Fig. 2c). Consequently, the landslide and its secondary disasters severely disrupted the reservoir operation because of the complete damage to radial gates, auxiliary structures, railing, and an emergency electrical generator.



Figure 2. (a) UAV's photo of the Van Hoi reservoir, (b, c) Photo of the slope after sliding and its extensive damage to the dam facilities on December 20, 2016 (Photos courtesy by Do Canh Hao), and (d, e) Sediment deposition reservoir floor took on October 4, 2019

The sediment deposition in the Van Hoi irrigation reservoir remains a severe issue, posing a threat to its functionality and life span due to limited budgets for implementing measures to address the accumulated soil mass (Figs. 2d, e). Notably, the dam reservoir is highly susceptible to landslides. Although the mass movement of the deep-seated Van Hoi landslide has received the attention and concerns of researchers and authorities, detailed studies on the landslide and its secondary hazard have been lacking. There is a need for a comprehensive understanding of the mechanism and processes involved in the Van Hoi rapid landslide. This research, therefore, aims to investigate the sliding mechanism and reproduce the entire sliding processes of the rainfall-induced landslide using integrated simulations utilizing the ring shear simulator and the LS-RAPID software. The computer modeling and understanding of the sliding mechanism during the 2016 disaster will provide valuable insights for future landslide hazard assessments of slopes in the Van Hoi reservoir area.

## 2. Materials and methods

First, we conducted site surveys to examine the landslide characteristics and the failed slope, including their dimensions, features, sliding surface, slope strata, and another reservoir topographical and morphological features utilizing a Phantom-4 Pro unmanned aerial vehicle (UAV). A digital elevation model (DEM) of the study area with 5 m resolution was created from UAV photos to present the terrain after the sliding (Fig. 3). The topographical data of the initial slope and sliding surface were derived from the UAV-generated DEM on-site measurement of the landslide features concerning the 5 m DEM provided by Vietnam Department of Survey and Mapping. During the site investigation,

intact and disturbed soil samples were collected along the sliding surface for laboratory experiments.

Then, the undrained ring shear simulator (ICL-2 version), which has a capacity of 3.0 MPa of normal stress, was employed to study the rapid deep-seated rainfall-induced landslide in the Van Hoi reservoir. The ring shear simulation enables quantitative observation of sample's failure, landslide formation and its motion at high velocities. It also facilitates monitoring changes in pore pressure and potential liquefaction during a steady-state large displacement (Sassa et al., 2004; Tien et al., 2017; Loi et al., 2018). The testing procedure with ICL-2 mainly consists of sample saturating, sample set, saturation parameter checking ( $B_D$ ), sample consolidation, and shearing. The initial step involved saturating the soil samples in a vacuum tank for several days. Subsequently, the saturated samples were placed in the apparatus box, which was saturated using carbon dioxide and de-aired water circulation to remove all air bubbles. The degree of saturation was indirectly examined using the  $B_D$ . The parameter ( $B_D = \Delta u / \Delta \sigma$ ) represents the ratio of increasing pore water pressure value to normal stress increment under undrained conditions (Sassa et al., 2010; Tien et al., 2018b). Undrained ring shear tests were consistently conducted with  $B_D \geq 0.95$ . Next, the initial stress state of the soil samples at their sliding surface was replicated under drained conditions. The initial normal and shear stresses ( $\delta_0 = \gamma \cdot h \cdot \cos^2 \theta$  and  $\tau_0 = \gamma \cdot h \cdot \cos \theta \cdot \sin \theta$ ) resulting from gravity were estimated based on the sliding depth ( $h$ ), soil unit weight ( $\gamma$ ), and slope angle ( $\theta$ ) (Tien et al., 2021b). In the final step, undrained tests were executed in different shearing modes. This research investigated the samples' strength characteristics and landslide mechanism in undrained shear displacement control tests (SDC tests). Undrained pore water pressure control test (PWP test) was

mainly performed to simulate the 2016 rain-induced landslide that occurred by the rising groundwater levels due to rainfall. For physical simulation, normal stress of 450 kPa

and shear stress of 170 kPa, which approximately correspond to the maximum landslide depth of 26.5 m, was applied in the laboratory experiments.

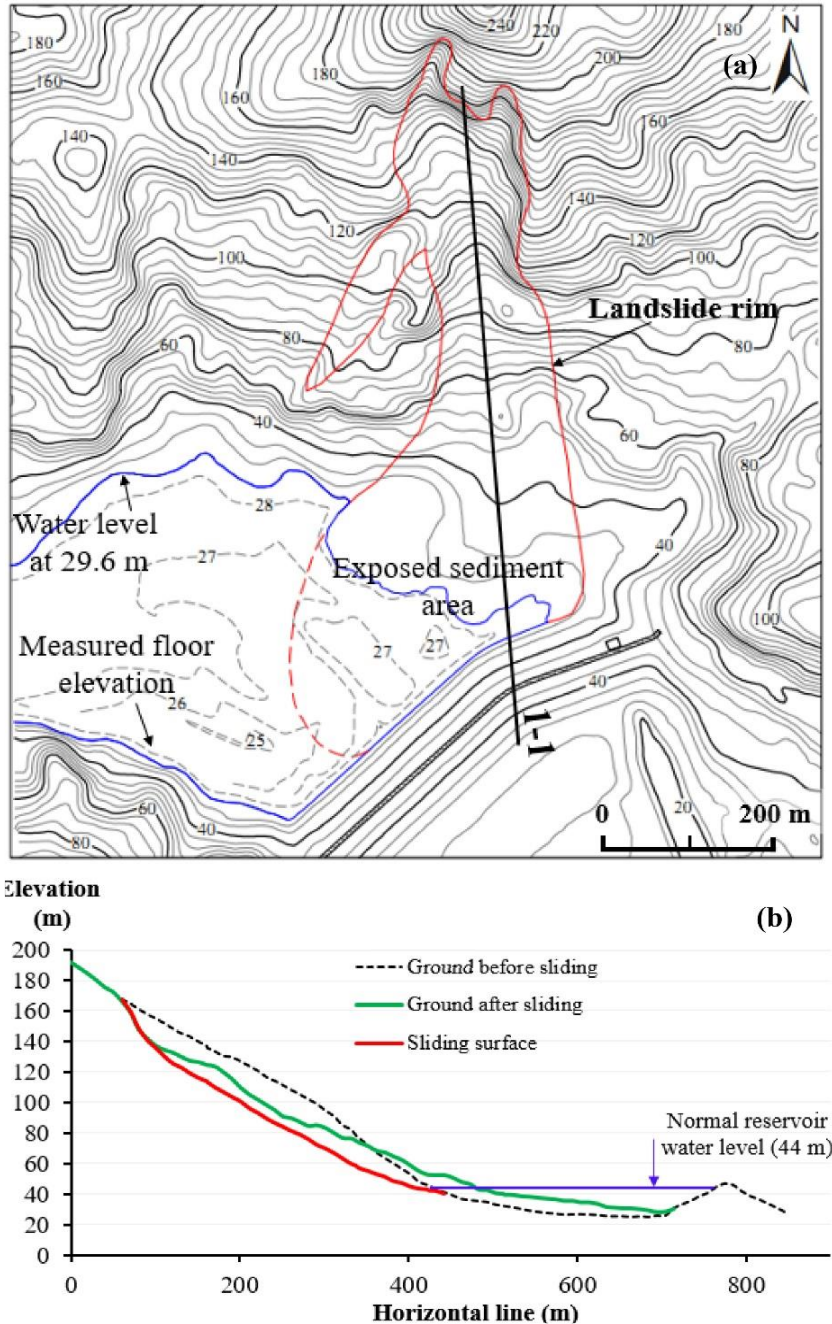


Figure 3. The largest deep-seated landslide at the Van Hoi reservoir: (a) the slope terrain after the event, and (b) a slope profile (1-1) showing the sliding plane and slopes before and after sliding

Finally, the Van Hoi deep-seated landslide's initiation and motion process was reproduced using the integrated LS-RAPID simulation software, which utilized key soil sample parameters obtained from the SDC and PWP experiments. The fundamental concept of LS-RAPID a three-dimensional continuum model, is to calculate all different types of forces acting on a displaced mass. These forces encompass the total weight of soil mass, lateral pressure, normal stress, shear resistance, pore pressure, and seismic forces. This LS-RAPID model integrates the landslide initiation caused by the build-up of pore water pressure and earthquake loads, the moving process due to strength loss, and the process of entrainment involving unstable material layers along the traveling way. The initiating and moving processes of landslides, recreated in the computer model, are exhibited from the stable condition to the failure and then reaching the post-failure phase at a steady condition (Sassa et al., 2010; Tien et al., 2018a and 2018b). The 5-meter DEM data was utilized both before and after the landslide event. In the simulation, the pore water pressure ratio ( $r_u$ ), which acted as a landslide triggering factor, was employed to simulate the rise of groundwater levels resulting from precipitation. Soil properties obtained from the undrained experiments were used as the key parameter for the LS-RAPID model, whereas some were approximately calculated based on the site surveys.

### 3. The deep-seated landslide and soil sampling

The Van Hoi reservoir is surrounded by medium and low-altitude mountains ranging from 105 to 740 m, covered by *Acacia mangium* trees. The largest deep-seated landslide is located at 14°24'3.17"N and 108°54'42.72"E on the left bank of the Van Hoi dam in Binh Dinh province (Fig. 1). The reservoir areas situated on the southern edge of Kontum Massif in Central Region of Vietnam, which impacted by tectonic

activities and the tropical monsoon climate. As shown in Fig. 1, the Van Hoi reservoir area is characterized by the intersection of Tong Dinh-Truong Xuan Fault (F1) and An Lao River Fault (F11). The geological setting is underlain by the Kim Son Formation, characterized by biotite-plagiogneiss and granat two-mica quartzite, and the Hai Van Complex with biotite granite and two-mica granite (Truong Khac Vy 2003). According to the site survey and DEM data analysis, the large landslide in the Van Hoi reservoir had a volume of 583.000 m<sup>3</sup> and failed on an area of 74.000 m<sup>2</sup>. The contour map of the study area and main cross-section of the landslide are shown in Fig. 3. The study area consisted of a central sliding mass on the left flank and the subsequent sliding part on the right side. The main landslide body, approximately 400 m in length, 145 m in width, and a maximum depth of 27 m, occurred on the moderate gentle hill slope of about 20.5°. The landslide initiated at an elevation of 172 m, rushed down the bank into the lake, and spread over a large area on the reservoir floor, reaching more than 400 m from the slope foot to the dam bottom, with a maximum soil thickness of 10 m. The sediment was mainly deposited near the spillway gate, seriously impacting the reservoir operation.

The Van Hoi deep-seated landslide was induced by intense rainfall at approximately 5:00 AM on December 16, 2016. Precipitation data monitored at the Hoai An and Hoai Nhon Meteorological stations, located near the landslide site, is shown in Fig. 4. Four continuous heavy rainfall events occurred from October 27 to December 21, 2016. Among them, twice rainfall events with extreme intensity took place from November 29 to December 9 and December 11 to 21, separated by no rainfall on December 10. The failed slope experienced consecutive 5-day heavy rainfall, with the daily precipitation ranging from 66.2 to 316 mm four days before the sliding event. The accumulated rainfall amounts recorded at the Hoai Nhon and Hoai

An stations were 1.992 mm and 1.948 mm from October 27 to December 16 (51 days) and 1.529 and 1.465 mm between November 29 to December 16 (18 days), respectively. Notably, 778 and 747.1 mm accumulative values were measured from December 11 to

16. The 1 day antecedent rainfall for the sliding event was 316.1 and 269.6 mm for the Hoai Nhon and Hoai An rain gauges. The rainfall data shows that prolonged intense rainfall was mainly the triggering factor for the Van Hoi mass movement.

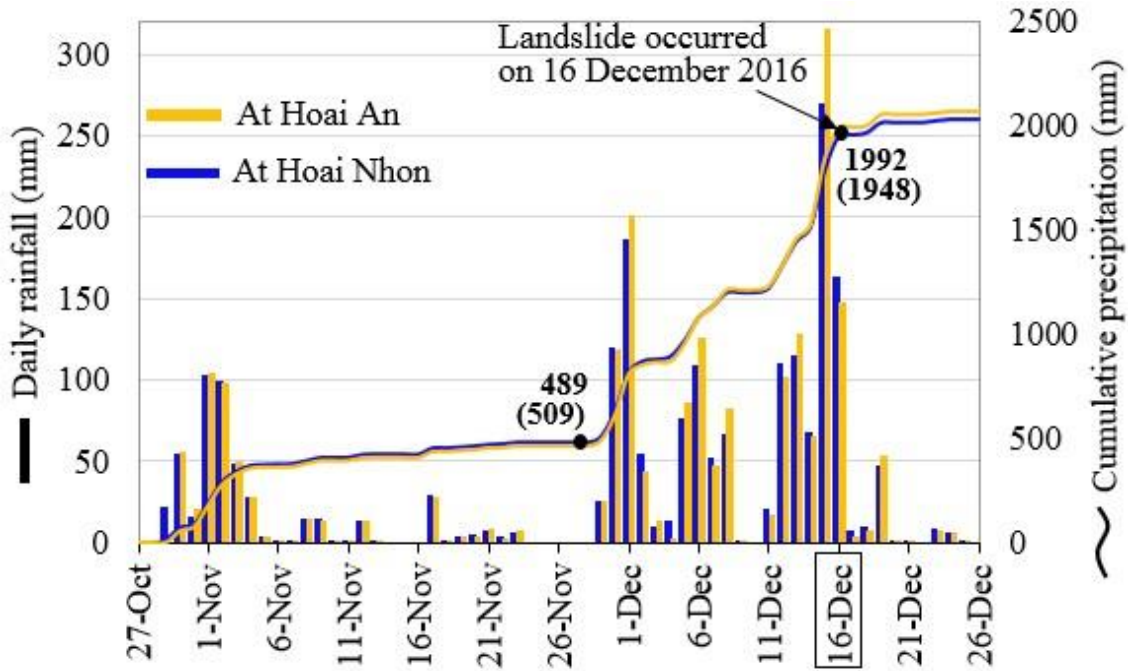


Figure 4. Daily rainfall and its accumulated precipitation before and after the sliding at Hoai Nhon and Hoai An meteorological stations from October 27 to December 26, 2016

The site surveys showed the landslide, characterized by a rotational type, occurred along the bedding surfaces of slightly to moderately weathered gneiss bedrock. The sliding plane was exposed in the displaced mass's left flank and head scarp (as shown in Figs. 5a and 5b). The landslide deposits mainly comprised of loose and completely weathered materials from gneiss rocks. The mechanical behavior of the sliding zone materials commonly controls the sliding mechanism (Tien et al., 2018b). Two soil samples along the sliding surface were collected for physical ring shear tests. The first sampling point is below the head scarp, which is silty sand

materials of residual soils (sample 1 or silty sand). The second sampling location is on the higher middle left flank of the landslide source, characterized by sandy materials of the completely weathered gneiss layer (sample 2 or sand sample). The unit weight of samples 1 and 2 calculated from laboratory tests was about 19.6 and 20.1 kN/m<sup>3</sup>, respectively. The photographs of the two soil samples and their respective grain-size distributions are denoted in Fig. 5c and Fig. 5d. The analysis of grain-size distribution indicated that sample 2 consisted of a large amount of sand-size grains. In contrast, sample 1 was considerably finer compared to sample 2.

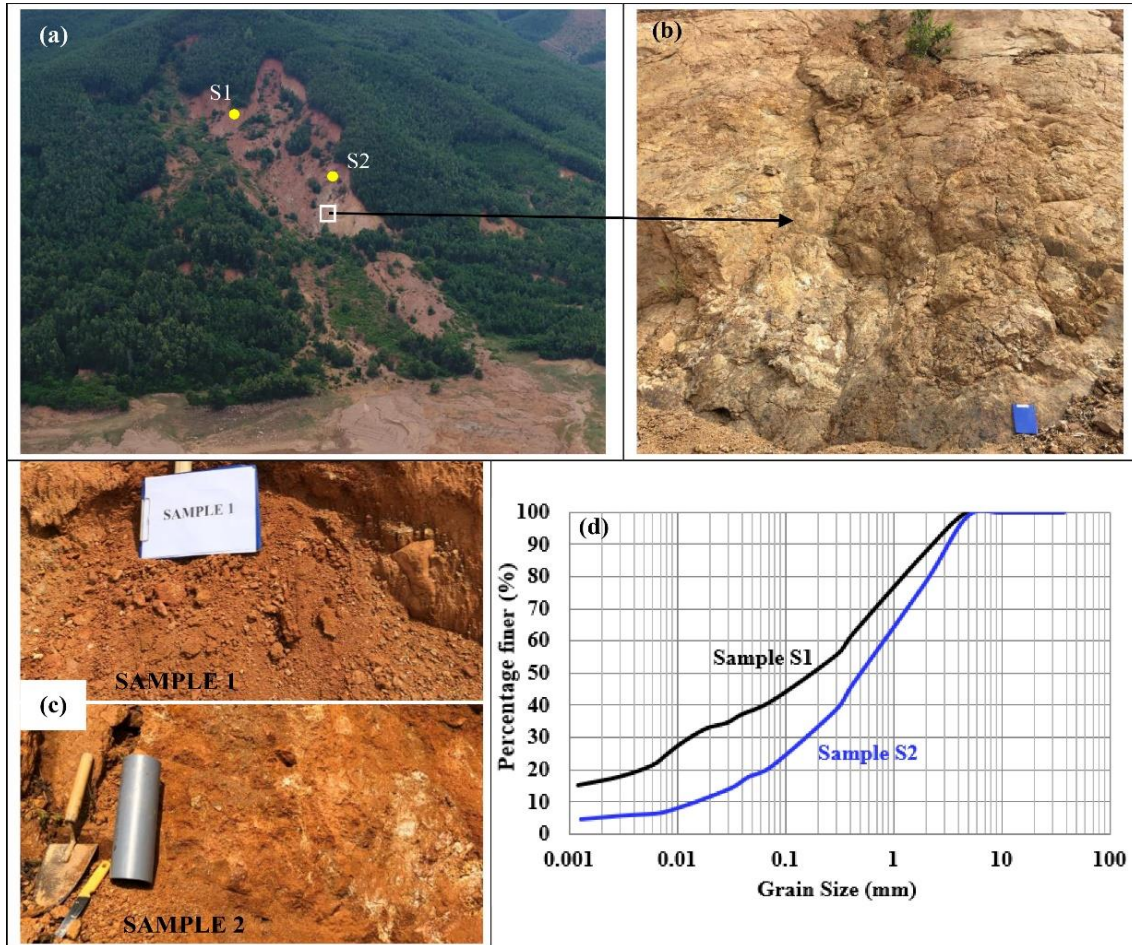


Figure 5. (a) Overview of the Van Hoi landslide body with sampling locations, (b) A closed-view of the sliding surface along the weathering gneiss rocks, (c) Photographs of soil samplings: silty sand material at point S1 (sample 1) and sand material at point S2 (sample 2), and (d) Grain-size distribution of samples 1 and 2

#### 4. Investigation of landslide mechanism with ring shear tests

##### 4.1. Undrained shear displacement control tests

Shear strength parameters of samples 1 and 2 were measured through the performance of SDC tests (Figs. 6, 7). After drained consolidation under normal stress of 450 kPa, samples 1 and 2 were subjected to shearing using a constant displacement rate of 1 mm/s and 2 mm/s in undrained conditions, respectively. The lower shearing speed was

applied to sample 1 because of its lower permeability. The shearing process continued until a shearing displacement of 3.500 mm was reached. The samples exhibited failure when the stress path intersected the failure line, subsequently, went down to the steady-state stress point along the failure line. Figure 6 illustrates the stress path and time series data of the SDC test for sample 1, with the mobilized friction angle at failure ( $\phi_p$ ) of  $42.3^\circ$ . The test revealed a high mobilized shear resistance at a steady state ( $\tau_{ss}$ ) of 212 kPa (Fig. 6a) and minimal pore water



pressure generation during shearing (Fig. 6b). These results suggest that sample 1 is unlikely to exhibit the mobile behavior of a rapid landslide.

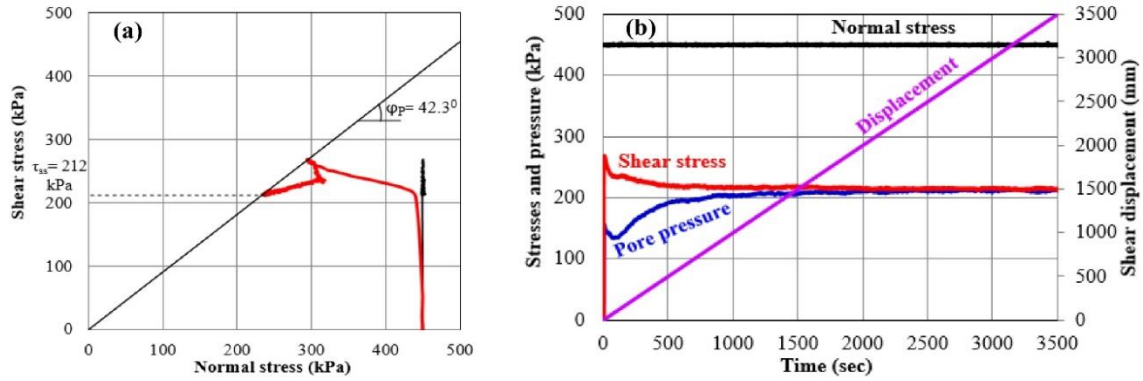


Figure 6. Result of USD tests on samples 1: (a) Stress path, and (b) Time series data

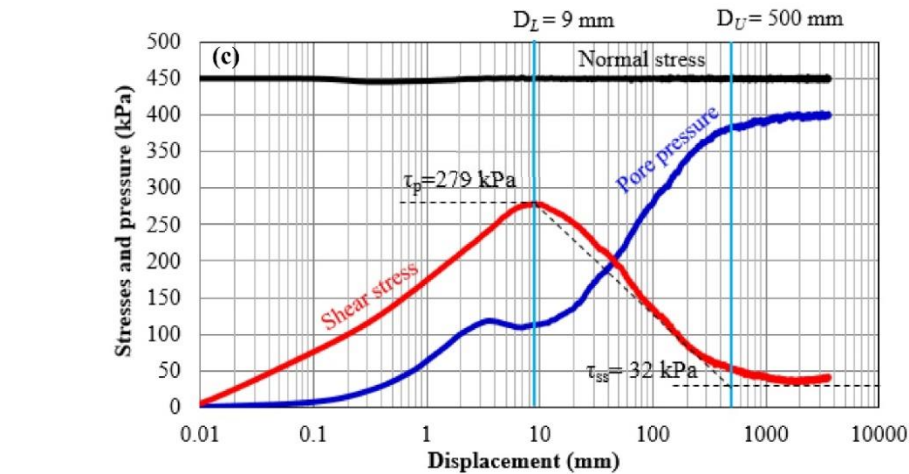
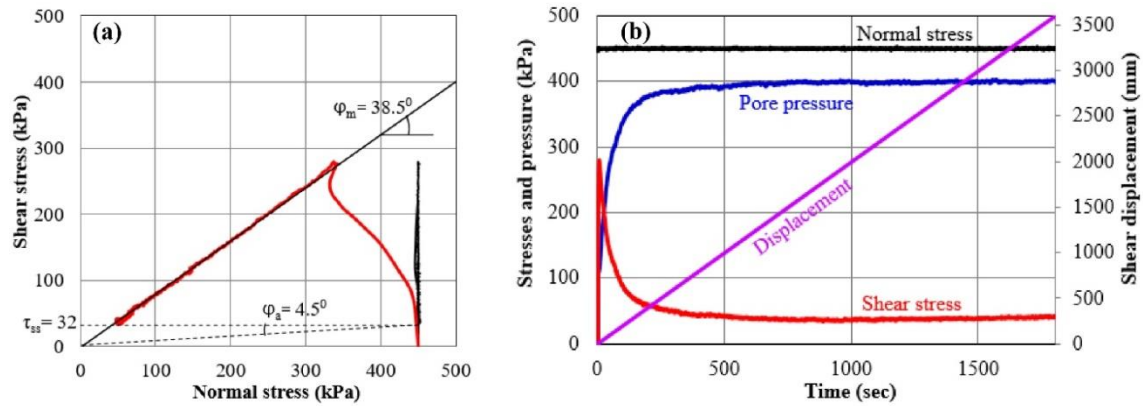


Figure 7. Result of USD tests on sample 2: (a) Stress path for sample 2, (b) Time series data, and (c) Shear stress in the progress of shear displacement

The monitored stress path and time series data of the SDC test for sample 2 are drawn in Figs. 7a and 7b. Immediately after the shearing loading, sample 2 failed under a small shear

displacement. As a result, the shear strength sharply decreased due to a build-up of a very high pore water pressure value generated from the incessant grain crushing of the sample. The shear path moved along the failure line to a low shear resistance value of 32 kPa at the steady state. The friction angle was measured  $38.5^\circ$  during motion, while the apparent friction angle mobilized at only  $4.5^\circ$ . Test results indicated the typical sliding surface liquefaction phenomena resulting in the rapid-moving landslide (Sassa et al., 2004; Tien et al., 2018b, 2021b). The sample failure was denoted by the following four distinct periods of pre-failure, failure, transient phase, and steady state (Fig. 7c). At peak strength; sample 2 failed at a critical shear displacement (shear displacement at the beginning of shear reduction,  $D_L$ ) of 9 mm. The shear displacement for initiating steady-state residual shear resistance ( $D_U$ ) was about 500 mm.

**4.2 Simulation of the Van Hoi rainfall-induced landslide with PWP test**

Considering the high mobility behavior exhibited by sample 2, which represents the rapid Van Hoi landslide, a simulation of the rainfall-induced landslide was conducted using a PWP test on sample 2 (Fig. 8). In this simulation, sample 2 was initially consolidated at normal stress and shear stress

of 450 and 170 kPa in the drained condition (black line in Fig. 8b), respectively. Subsequently, the pore water pressure value was increased at a designed rate of 1 kPa/s until it reached the point of failure to simulate the groundwater level rise due to the rainfall infiltration process. The test was turned into an undrained condition at the failure point by closing the drainage valve. The test results on sample 2 are presented in Fig. 8. The landslide occurrence was observed when the stress path shifted to the failure line. The friction angle at the peak was  $41.6^\circ$  for the PWP test. The failure of sample 2 was triggered by pore water pressures of 265 kPa, corresponding to a critical ratio of pore water pressure ( $r_u$ ) of 0.59. Here, the parameter  $r_u$  is calculated as the ratio between the increment of pore pressure that triggers failures and the normal stress. In this PWP simulation, the experiment was terminated at a shear displacement of 10 m. Remarkably, the rapid motion of sample 2 was observed during the rainfall-induced landslide simulation. This behavior can be attributed to liquefaction behavior within sliding surface of sample 2, which is caused by a rapid development of excess pore water pressure resulting in a significant soil strength loss. The shear strength of sample 2 mobilized at a low value of steady-state residual strength and apparent friction angle.

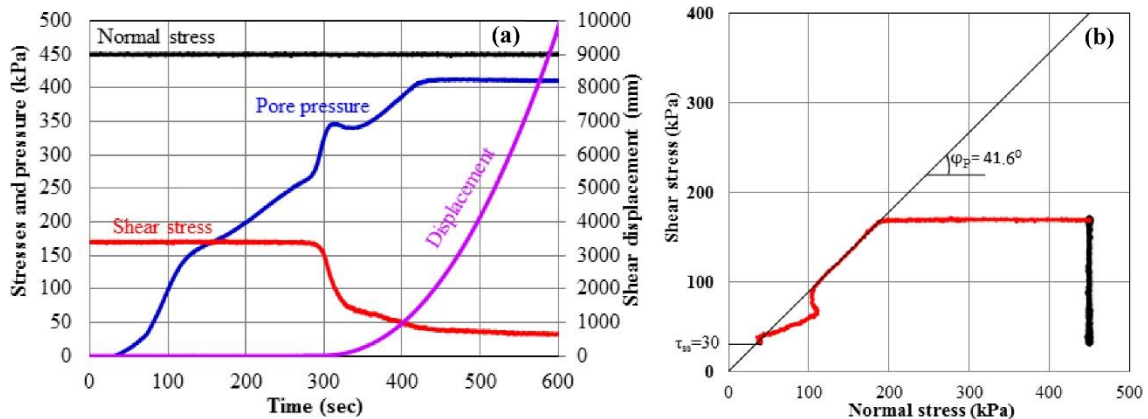


Figure 8. PWP test for rainfall-induced landslide on sample 2: (a) time series data and (b) effective stress path

### 5. The simulation of the Van Hoi landslide with LS-RAPID model

The computer simulation of the rapid and deep landslide in the Van Hoi reservoir was performed in the LS-RAPID model. Based on the findings mentioned earlier, the high mobility of the Van Hoi landslide was mainly attributed to the shear behavior of sample 2. Thus, the soil parameters obtained in the laboratory experiment on sample 2 were applied to the model. Besides, the model employed the pore pressure ratio, representing the increase in groundwater level due to rainfall, as a triggering factor for the landslide. The geotechnical parameters used in the LS-RAPID model are shown in Table 1, along with a detailed explanation of essential input parameters:

- Lateral pressure ratio ( $k$ ): The  $k$ -value was estimated to be 0.7 in the sliding area and 0.9 for the reservoir base.

- $D_U$  and  $D_L$  values: The critical shear displacement ( $D_L$ ) and ( $D_U$ ) were 9 mm and 500 mm, respectively (Fig. 7c).

- Steady-state shear strength ( $\tau_{ss}$ ): A residual shear strength of 30 kPa was input into the model. A lower value of 10 kPa was assumed for the area beneath the reservoir water level.

- Excess pore water pressure generation ( $B_{ss}$ ): The value  $B_{ss}$  varied based on the saturation level of the slope, which was influenced by the groundwater level. Values of 0.6, 0.8, and 0.9 were assigned to the upper parts, middle slope, and lower part of the slope, respectively. A value of 0.98 was set to the reservoir base.

- Pore pressure ratio ( $r_u$ ): The testing models initially used the pore pressure ratio of 0.59 obtained in the rainfall-induced landslide simulation by ring shear test. However, it was found that the critical value triggering the Van Hoi landslide was 0.55 after carefully doing validation and calibration. Therefore,  $r_u = 0.55$  was used as a critical pore pressure ratio with a time increment of 30 seconds.

- Non-friction energy consumption coefficient:  $\alpha = 5$  (according to Sassa et al., 2010).

The evolution process of the rapid rain-induced landslide in the Van Hoi irrigation reservoir is presented in Fig. 9. In the model, the red ball zones indicate unstable parts where failures occur. The slope remained stable when the ratio of pore water pressure reached 0.54 at 29 seconds (Fig. 9a). At 30 seconds, local failures (represented by red points) occurred when the ratio attained a critical value of  $r_u = 0.55$  (Fig. 9b). The ratio value of  $r_u = 0.55$  was maintained from the 30<sup>th</sup> second until the end of the simulation.

The local failures initially started in the middle slope of the main sliding area and then expanded to adjacent areas in both the upper and lower parts. The upper areas slid due to losing support at its base. In the motion progress, the overriding of upper sliding parts on their lower zone triggered the lower slope movement under the dynamic effects (Fig. 9c). This mechanical process rapidly continued and exacerbated the failure on the slope. The slope rushed down to the reservoir water surface at 48.0 seconds (Fig. 9d). The high-speed movement was accelerated due to a suddenly shear strength reduction of sliding materials and rapid build-up of pore water pressure within the sliding surface (Fig. 9e-g). As shown in Fig. 9e, the maximum speed of the Van Hoi landslide was approximately 37 m/s. After rapid downslope movement, the debris mass collided with the dam structure and spread back into the reservoir base areas. Finally, the sliding zone expanded to a large slope, and the landslide motion stopped at 122.4 seconds (Fig. 9h). Fig. 10 presents the model result and a comparison of the topographical data of the landslide. The modeling results closely resembled the landslide-affected zone depicted by UAV-based DEM data and on-site evidence. In addition, the location of the initial failure in the Van Hoi landslide was derived from the middle zone of the slope, where other mass movements were taken place in the study site on December 16, 2016. This model result is reasonable considering the similarity in geological and hydrological settings in a small-scale slope area.

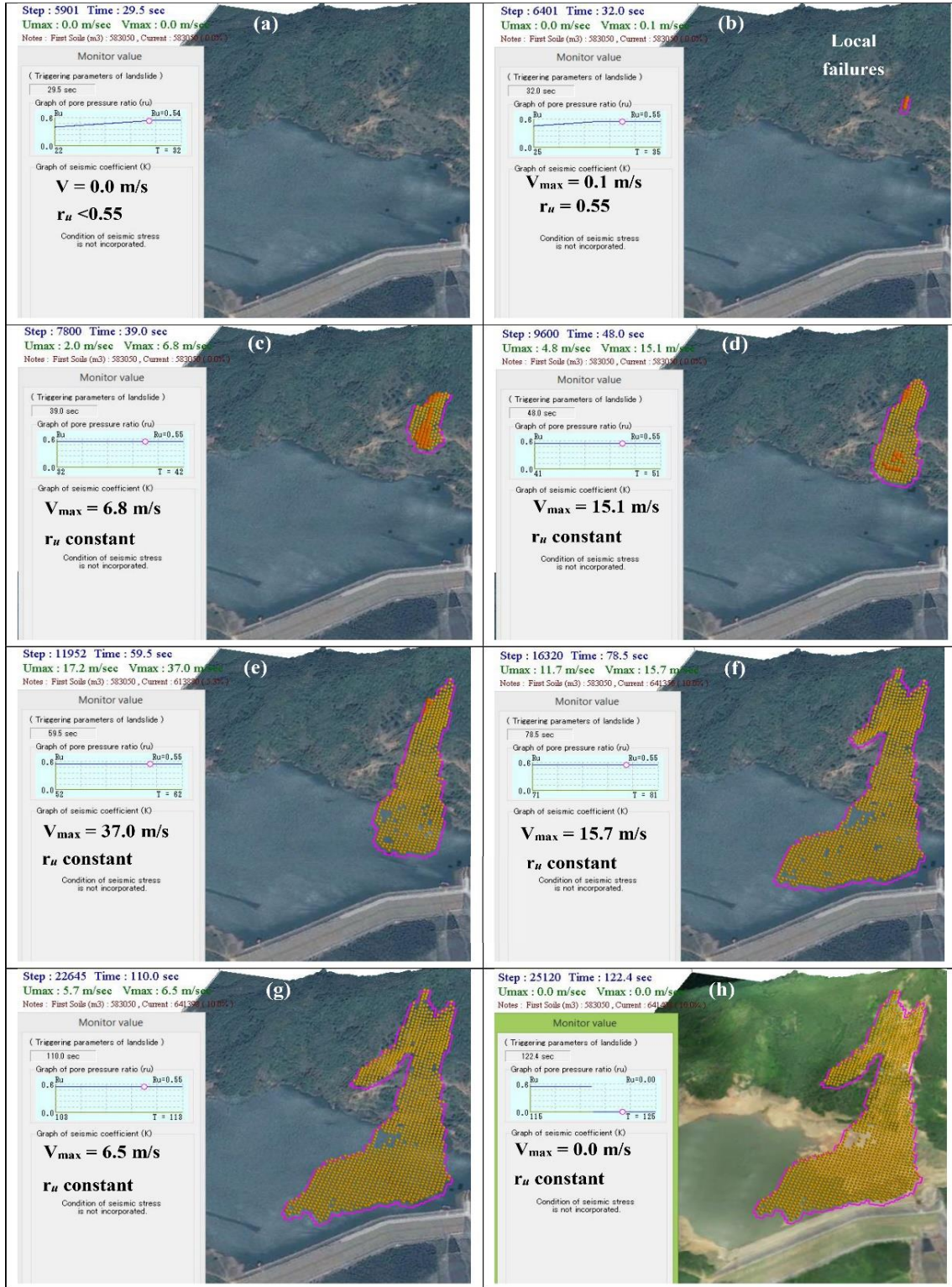


Figure 9. Entire initiation and motion process of the Van Hoi landslide

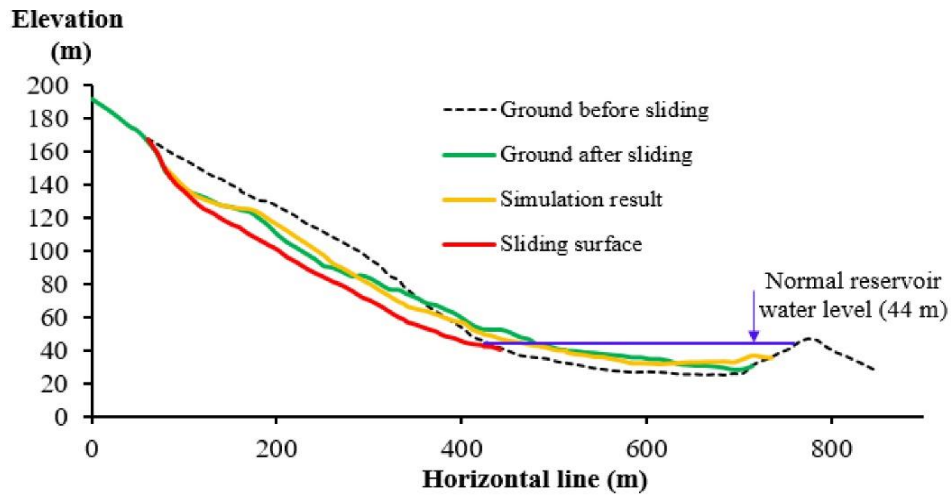


Figure 10. Comparison of the ground surface after sliding in 2016 and its elevation drawn from the LS-RAPID model

Table 1. Soil parameters for the computer simulation model

Soil parameters	Value	Source
Unit weight of the mass ( $\gamma_s$ , kN/m <sup>3</sup> )	19.6	Experiment data
Unit weight of water ( $\gamma_w$ , kN/m <sup>3</sup> )	9.81	Assumed
Lateral pressure ratio ( $k = \sigma_h/\sigma_v$ )	0.4-0.7	Estimated
Pore pressure generation rate ( $B_{ss}$ )	0.55-0.75	Estimated
Friction angle during motion ( $\phi_m$ , degree)	38.5	Experiment data
Peak friction angle ( $\phi_p$ , degree)	41.5	Experiment data
Steady-state shear resistance ( $\tau_{ss}$ , kPa)	30	Experiment data
Shear displacement at the start of strength reduction ( $D_{L_s}$ , mm)	9	Experiment data
Shear displacement at the end of strength reduction ( $D_{L_e}$ , mm)	500	Experiment data
Critical pore pressure ratio ( $r_u$ )	0.55	Experiment data

## 6. Discussions

Located in the tropical monsoon climate region with intense cleavage terrain and complex geological structures, Vietnam is one of Southeast Asia's most prone to landslide hazards. Landslides frequently occur during tropical cyclones in rainy seasons, causing significant damage and fatalities (An, 2010; Thien and Ly, 2013; Hung 2014; Hung and Huyen, 2015; Tien et al., 2015; Tien et al., 2016a, 2016b; Dieu et al., 2017; Luong et al., 2016, 2017; Lan et al., 2019; Tien et al., 2021a, 2021d). The Van Hoi large landslide was induced by prolonged heavy rainfall on December 16, 2016, in Binh Dinh province in Central Vietnam. The landslide, approximately 583,000 m<sup>3</sup> in volume, slid

along the bedding planes of weathered gneiss bedrock. The rapid movement of the Van Hoi landslide into the reservoir induced a high tsunami wave and caused severe damage to the dam facilities and its reservoir operation. A large volume of landslide debris material was deposited on the lake base, which reduced the storage capacity and exacerbated the sedimentation problem. Two heavy rainfall events from November 29 to December 9 and December 11 to 21 were recognized as critical factors in the sliding. The accumulated amounts at the Hoai Nhon and Hoai An stations were 1.529 mm and 1.465 mm, respectively, over 18-day from November 29 to December 16. The detailed investigation indicates that high-intensity and long-duration

rainfall was the primary triggering factor for the deep-seated landslide. The prolonged heavy rainfall triggering the landslide is a typical pattern that frequently occurs in Central Vietnam during the rainstorm seasons (Hung and Dung, 2013; Tien et al., 2021a, 2021e). Under extremely heavy rainfall, rainwater infiltration increased the weight of soil mass and the saturation degree of the slope, resulting in a significant decrease in shear resistance. Notably, it also led to a rise in groundwater level and pore water pressure, which triggered the failure.

The SDC and PWP tests were conducted on the two collected soil samples to investigate the physical mechanism of the 2016 Van Hoi landslide. Test results indicate that only sample 2 exhibited immediate excess pore water pressure generation during early shear displacement. As shearing progressed, the shear strength of sample 2 suddenly dropped in the increasing progress of shear displacement. This drop was predominantly attributed to the generation of high pore water pressure, which was caused by incessant grain crushing during shearing in the shear zone. These observations indicate that sample 2 was characterized by sliding surface liquefaction phenomena, which shows extensive grain crushing behavior, rapid pore pressure development, and a significant strength loss (Sassa et al., 2004; Sassa et al., 2010; Tien et al., 2018b, 2021b). This feature is typical for granular materials of sample 2, which consist of sand and are highly susceptible to rapid landslides.

Conversely, sample 1 was not subjected to excess grain crushing because of its fine-grained mineral and did not produce a high pore pressure value. The results pointed out that the mobility behavior of sample 2 mainly governed the mechanism of the 2016 rapid landslide, and the sliding surface was likely formed in the completely weathered gneiss layers. Using the soil parameter measured

from geotechnical ring shear tests, the computer model successfully replicated the Van Hoi landslide, exhibiting a maximum velocity of 37.0 m/s during travel. The rapid landslides are the most dangerous because of the potential for extensive destruction. The study finding provides valuable insight into hazard assessment of rapid-moving landslides that commonly take place in Vietnam and other countries (Loi et al., 2017; Tien et al., 2017; Tien et al., 2018b; Loi et al., 2018; Tien et al., 2021a, 2021e).

An undrained PWP test was implemented to indirectly investigate the effect of change in the groundwater table and reproduce the Van Hoi deep-seated landslide. The pore water pressure ratio measured in the test was one of the most important input parameters in the computer simulation. The downslope movement is initiated at a critical pore water pressure ( $r_u$ ) value of 0.55. The simulation presented the crucial factor of a high pore water pressure resulting in slope movement. Although hydrological monitoring data was unavailable at the study site, the calculated value of pore water pressure suggested a high groundwater table during rainfall, which triggered the Van Hoi landslide. A similar condition of high groundwater level caused the slow-moving landslide was also presented at the Tan Son landslide area in Ha Giang province (Duc et al., 2023). It is highly recommended that the pore water pressure value (the  $r_u$  ratio), which describes the geotechnical behavior of soils under different loadings (Tien et al., 2018a, 2018b; Nhan et al., 2021, 2022), can be used as an appropriate parameter for an early warning system for landslide hazards. Based on this examination, a real-time monitoring system comprising rainfall gauges and pore pressure transducers can be installed in the Van Hoi reservoir area for landslide hazard prediction and mitigation. In addition, a successful simulation of the Van Hoi landslide case using the integrated

landslide simulation model can provide an effective and reliable tool for hazard and risk assessment of various rainfall-induced deep-seated landslides that frequently occur during the tropical rainy season in Vietnam, such as the 2020 deadly rapid landslide in Rao Trang-3 and 4 hydropower plant area, in Thua Thien Hue province and the 2020 deadliest single landslide event in Quang Tri province (Tien et al., 2021a, 2021e).

## 7. Conclusions

This paper interprets the rapid and deep landslide mechanism and sliding process caused by intense rainfall in the Van Hoi reservoir water surface area in Binh Dinh province, Vietnam. The significant findings of the study are summarized as below:

- The test results indicated that the failure mechanism of the rapid landslide dominantly depended on the shearing behavior of sample 2 collected along the sliding surface. In the tests, only sample 2 experienced sliding surface liquefaction followed by extensive grain crushing, excess pore water pressure development, and significant soil strength loss during a large shear displacement. It had a low mobilized friction angle and residual strength at a steady state. This behavior implies that sample 2 was the causative factor for rapid landslide movement, and the Van Hoi mass movement could occur in this material layer. In contrast, sample 1 did not exhibit the same propensity for rapid landslides due to a low level of grain crushing and a limited generation of pore water pressure.

- The heavy and prolonged rainfall was the primary factor that triggered the landslide event on December 16, 2016. The 18-day antecedent rainfall had a high accumulated amount of 1.529 mm and 1.465 mm at the Hoai Nhon and Hoai An stations, respectively. The PWP test simulating rainfall-induced landslide indicates that the landslide was

initiated due to high excess pore pressure generation and significant shear strength reduction. The rapid motion of the landslide was observed during the simulation.

- The LS-RAPID model successfully reproduced the Van Hoi landslide initiation and motion process. The Van Hoi landslide was induced by a high accumulative precipitation with a critical pore pressure ratio  $r_u = 0.55$ . The rapid mass movement traveled at a high velocity of 37 m/s for a long distance on the reservoir base and finally deposited along the dam toe. The model utilized physically input parameters obtained from physical experiments and was examined as closely as possible with actual sliding processes, on-site evidence, and recorded data.

The integrated approach utilizing ring shear apparatus and computer simulation model (LS-RAPID) effectively investigated the mechanism and simulated the rainfall-induced rapid and deep-seated landslide processes. The Van Hoi landslide's formation mechanism has not been examined since its occurrence. Thus, the findings of this research are helpful for hazard assessment of compound landslides in Van Hoi to better prepare for possible future disasters.

## Acknowledgments

This research is funded by Vietnam National Foundation for Science and Technology Development (NAFOSTED) under grant number 105.08-2019.14. We want like to thank MSc. Do Canh Hao (Institute of Training and Science Application, Thuyloi University); Assoc. Prof. Do Dinh Toat (Institute of Geotechnology and Environment); Prof. Do Minh Duc (VNU University of Science, Vietnam National University) and Dr. Bui Van Thom and Mr. Tran Trung Hieu (Institute of Geological Sciences, Vietnam Academy of Science and Technology) for their valuable assistance in this study. In particular, the authors are

immensely grateful to Dr. Ngo Quoc Kim Long (DJI Enterprise, Vietnam) for his essential support to the UAV field investigation. The insightful comments and suggestions of the Editors and two anonymous reviewers are gratefully acknowledged.

## Reference

- An L.D., 2010. A method for study of rainfall thresholds for landslide warning. *Vietnam J. Earth Sci.*, 32(2), 97-105.
- An T.T.P., Matsuda H., Nhan T.T., Nhan N.T.T., Tien P.V., Thien D.Q., 2021. Pore water pressure responses of saturated sand and clay under undrained cyclic shearing. *Vietnam J. Earth Sci.*, 44(2), 181-194.
- Duc D.M., Minh V.C., Yen H.H., Loc N.T., Duc D.M., 2023. Analysis of landslide kinematics integrating weather and geotechnical monitoring data at Tan Son slow moving landslide in Ha Giang province. *Vietnam J. Earth Sci.*, 45(2), 131-146.
- Hoang N.V., Khang U.Q., 2011. Rainwater infiltration modelling for slope stability analysis in Coc Pai town-Xin Man district-Ha Giang province. *Vietnam J. Earth Sci.*, 33(1), 78-84.
- Hung P.V., Dung N.V., 2013. Risk warning landslide in the mountainous districts of Quang Ngai province. *Vietnam J. Earth Sci.*, 35(2), 107-119.
- Hung P.V., 2014. Risk assessment of damage caused by landslide in the mountainous districts of Quang Ngai province. *Vietnam J. Earth Sci.*, 36(2), 108-120.
- Hung P.V., Huyen N.X., 2015. The risk assessment of loss due to landslides-cracks in the Tay Nguyen. *Vietnam J. Earth Sci.*, 37 (2), 148-155.
- Lan C.N., Tien P.V., Do T.N., 2019. Deep-seated rainfall-induced landslides on a new expressway: a case study in Vietnam. *Landslides*, 17(2), 395-407.
- Loi D.H., Quang L.H., Sassa K., Takara K., Khang D., Thanh N.K., Tien P.V., 2017. The July 28 2015 rapid landslide at Ha Long city, Quang Ninh, Vietnam. *Landslides*, 14, 1207-1215.
- Loi D.H., Sassa K., Fukuoka H., Sato Y., Takara K., Setiawan H., Tien P.V., Khang D., 2018. Initiation Mechanism of Rapid and Long Run-Out Landslide and Simulation of Hiroshima Landslide Disasters Using the Integrated Simulation Model (LS-RAPID). *Landslide Dynamics: ISDR-ICL Landslide Interactive Teaching Tools*, Springer International Publishing, 149-168.
- Luong L.H., Miyagi T., Tien P.V., 2016. Mapping of large scale landslide topographic area by aerial photograph interpretation and possibilities for application to risk assessment for the Ho Chi Minh route-Vietnam. *Transactions, Japanese Geomorphological Union*, 97-118.
- Luong L.H., Miyagi T., Tien P.V., Loi D.H., Hamasaki E., Abe S., 2017. Landslide risk evaluation in central provinces of Vietnam. *Advancing Culture of Living with Landslides*, 1145-1153.
- MARD, 2005. Guide for Operational Safety of Van Hoi Irrigation Reservoir, Binh Dinh province. The Ministry of Agriculture and Rural Development (MARD) - Vietnam.
- Nhan T.T., Matsuda H., An T.T.P., Nhan N.T.T., Tien P.V., Thien D.Q., 2022. Effects of physical properties and undrained cyclic shear conditions on the pore water pressure responses of saturated sands and clays. *Vietnam J. Earth Sci.*, 45(1), 33-48.
- Sassa K., Dang K., He B., Takara K., Inoue K., Nagai O., 2014. A new high-stress undrained ring-shear apparatus and its application to the 1792 Unzen-Mayuyama megaslide in Japan. *Landslide*, 11(5), 827-842.
- Sassa K., Nagai O., Solidum R., Yamazaki Y., Ohta H., 2010. An integrated model simulating the initiation and motion of earthquake and rain induced rapid landslides and its application to the 2006 Leyte landslide. *Landslides*, 7(3), 219-236.
- Sassa K., Wang G., Fukuoka H., Wang F., Ochiai T., Sugiyama M., Sekiguchi T., 2004. Landslide risk evaluation and hazard zoning for rapid and long-travel landslides in urban development areas. *Landslides*, 1, 221-235.
- Tan M.T., Tao N.V., 2014. Studying landslides in Thua Thien - Hue province. *Vietnam J. Earth Sci.*, 36(2), 121-130.
- Tien P.V., Luong L.H., Duc D.M., Trinh P.T., Quynh D.T., Lan N.C., Thuy D.T., Phi N.Q., Cuong T.Q., Khang D., Loi D.H., 2021a. Rainfall-Induced Catastrophic Landslide in Quang Tri Province: the



- Deadliest Single Landslide Event in Vietnam in 2020. *Landslides*, 18(6), 2323-2327.
- Tien P.V., Luong L.H., Nhan T.T., Duc D.M., Quynh D.T., Lan N.C., Phi N.Q., Hao D.C., Ha N.H., Thuy D.T., 2021c. Secondary Processes Associated with Landslides in Vietnam. *Proceedings of the International Conference on Innovations for Sustainable and Responsible Mining, LNCE*, 108, 192-209.
- Tien P.V., Luong L.H., Nhat L.M., Thanh N.K., Cuong P.V., 2021d. Landslides along Halong-Vandon Expressway in Quang Ninh province, Vietnam. *Understanding and Reducing Landslide Disaster Risk*, 133-139.
- Tien P.V., Luong L.H., Sassa K., Takara K., Sumit M., Nhan T.T., Khang D., Duc D.M., 2021b. Mechanisms and modeling of the catastrophic landslide dam at Jure Village, Nepal. *J. Geotech. Geoenviron. Eng.*, 147(11), 05021010.
- Tien P.V., Sassa K., Takara K., 2016a. Study on Landslides in Weathered Granite Areas of Haivan Mountain, Vietnam. *Disaster Prevention Research Institute Annuals*, 59(B), 135-144.
- Tien P.V., Sassa K., Takara K., Fukuoka H., Khang D., Shibasaki T., Hendy S., Ha N.D., Luong L.H., 2018b. Mechanism of large-scale deep-seated landslides induced by rainfall in gravitationally deformed slopes: A case study of the Kuridaira landslide in Kii Peninsula. *Landslide Dynamics: ISDR-ICL Landslide Interactive Teaching Tools*, Springer International Publishing, 793-806.
- Tien P.V., Sassa K., Takara K., Fukuoka H., Khang D., Shibasaki T., Setiawan H., Ha N.D., Loi D.H., 2018a. Formation process of two massive dams following rainfall-induced deep-seated rapid landslide failures in the Kii Peninsula of Japan. *Landslides*, 15(9), 1761-1778.
- Tien P.V., Sassa K., Takara K., Khang D., Ha N.D., Luong L.H., 2017. Simulating the Formation Process of the Akatani Landslide Dam Induced by Rainfalls in Kii Peninsula, Japan. *Advancing Culture of Living with Landslides*, 497-506.
- Tien P.V., Sassa K., Takara K., Tam D.M., Quang L.H., Khang D., Luong L.H., Loi D.H., 2016b. The influence of rainfalls on the potential of landslide occurrence on Hai Van Mountain in Vietnam. *Proceeding of the Final SATREPS Workshop on Landslides*, October 13 Hanoi, Vietnam, 112-121, ISBN: 978-4-9903382-3-7.
- Tien P.V., Trinh P.T., Luong L.H., Nhat L.M., Duc D.M., Hieu T.T., Cuong T.Q., Nhan T.T., 2021e. The October 13, 2020 deadly rapid landslide triggered by heavy rainfall in Phong Dien, Thua Thien Hue, Vietnam. *Landslides*, 18(6), 2329-2333.
- Truong Khac Vy, 2003. *Geological Map of Binh Dinh areas (the Bong Son sheet at 1:50.000 scale)*. Department of Geology and Minerals of Vietnam.
- W.B., 2022. *Report on Environmental and Social Impact Assessment for Improving Flood Control Capacity for Large Reservoirs, Vietnam - Dam Rehabilitation and Safety Improvement Project: Environmental Assessment*. The World Bank, Ha Noi, 52, 270p.